

# Experimental confirmation of osteoarthritis repair *in vivo* using epigenetic reprogramming with small molecules

Saodat A. Muratkhodjaeva<sup>a</sup>, Javdat N. Muratkhodjaev<sup>a,\*</sup>, Tamara U. Aripova<sup>a</sup>

<sup>a</sup> Institute of Immunology and Human Genomics Academy of Sciences of Uzbekistan, Tashkent, 100060, Uzbekistan.

## Abstract

**Background:** Osteoarthritis (OA) is a progressive degenerative joint disease that significantly impairs mobility and quality of life, particularly in aging populations. Current therapeutic approaches primarily focus on symptom relief but fail to address the underlying mechanisms of cartilage degeneration. In recent years, epigenetic reprogramming has emerged as a promising strategy for cellular rejuvenation, offering new perspectives for regenerative medicine.

**Objective:** This study aimed to evaluate the effectiveness of small chemical molecules (SCM) in epigenetic reprogramming for the treatment of osteoarthritis (OA) in an aging organism.

**Design:** A preclinical study was conducted using female *Rattus norvegicus albinus* rats (age > 2 years, weight 250–270 g) with induced OA. The postmenopausal state was simulated via the estrogen receptor blocker clomiphene citrate. SCM were administered at concentrations previously established for *in vitro* epigenetic reprogramming. Histological and histochemical analyses of knee joint tissues were performed using hematoxylin and eosin, Van Gieson, and PAS staining. Cartilage degeneration was assessed using the modified Mankin scale. Statistical analysis included Student's t-test and correlation analysis.

**Results:** SCM administration resulted in a significant increase in tibial epiphyseal cartilage thickness and enhanced mucopolysaccharide synthesis, indicating metabolic activation of aging chondrocytes. Nuclear-cytoplasmic index changes in mitotically active cartilage regions suggested epigenetic rejuvenation, particularly in the superficial and intermediate zones. Notably, the response to SCM varied depending on estrogen receptor blockade. Rats with OA and induced menopause receiving SCM demonstrated the most pronounced cartilage regeneration, whereas untreated postmenopausal OA groups exhibited the most severe histological deterioration.

**Conclusion:** The study confirms the potential of SCM for epigenetic reprogramming in age-related OA, leading to cartilage regeneration and metabolic activation of chondrocytes without oncogenic risks. The findings highlight the need for further investigation into the interaction between estrogens and epigenetic rejuvenation, which may have implications for OA treatment in postmenopausal women.

**Keywords:** Epigenetic reprogramming, chondrocyte rejuvenation, osteoarthritis, small chemical molecules, cartilage regeneration

## Introduction

Aging is a complex biological process characterized by the gradual decline of tissue and organ function. Among

the various theories of aging, the epigenetic theory plays a key role, proposing that the accumulation of changes in the cellular epigenetic profile—such as DNA methylation and histone modifications—leads to dysregulation of gene expression essential for maintaining tissue homeostasis [1–5]. These changes are particularly critical in tissues with low regenerative capacity, such as articular cartilage, where epigenetic dysregulation has been implicated in the progression of osteoarthritis (OA) [6, 7]. OA is the most common joint disease, significantly reducing quality of life, especially in older individuals. Its pathogenesis involves hyaline cartilage degradation, chronic inflammation, and synovitis [8, 9]. One of the major risk factors for OA in women is postmenopausal estrogen deficiency,

\* Corresponding author: Javdat N. Muratkhodjaev  
Mailing address: International relations department, Institute of Immunology and Human Genomics Academy of Sciences of Uzbekistan, Tashkent, Y. Gulamov str. 74, 100060, Uzbekistan.  
E-mail: javdat\_m@yahoo.com

Received: 18 June 2025 / Revised: 09 July 2025

Accepted: 20 August 2025 / Published: XX September 2025

which exacerbates inflammatory and degenerative processes in cartilage and accelerates disease progression [10, 11].

Current therapeutic approaches primarily aim to relieve pain and improve joint function but fail to prevent disease progression or address its underlying causes [12–14]. As a result, strategies targeting epigenetic reprogramming of chondrocytes—the primary cells responsible for maintaining cartilage integrity—are gaining increased attention [15]. Several studies have demonstrated the potential of epigenetic rejuvenation in cell cultures undergoing replicative senescence, using small chemical molecules (SCMs) [16, 17]. These molecules modulate key epigenetic mechanisms, including chromatin remodeling and DNA methylation, thereby restoring a transcriptional profile characteristic of a more youthful cellular state. *In vitro*, epigenetic modifiers have been shown to enhance cell proliferation and reduce the expression of pro-inflammatory markers [18, 19].

While most evidence to date comes from *in vitro* systems, there is a growing need to validate these findings *in vivo*, particularly in the context of degenerative diseases such as OA. To address this, we developed a preclinical rat model of age-related OA to assess the regenerative potential of intra-articularly administered SCMs. To better simulate the human condition, we selected female rats over two years of age, roughly equivalent to humans over 60. This choice was based on their accelerated aging profile and the high relevance of postmenopausal OA in women. The model allowed investigation of epigenetic interventions in a physiologically relevant setting within a manageable experimental timeframe. To further explore the role of hormonal status, we used the estrogen receptor blocker clomiphene citrate. As previously demonstrated [20], this agent effectively induces postmenopausal conditions in rats. Compared to surgical ovariectomy, this pharmacological method offers the advantage of preserving animal mobility and reducing potential confounding effects on study outcomes. Estrogen receptors mediate hormonal effects across various tissues [21–23], and their blockade enabled assessment of the interaction between SCM-induced epigenetic reprogramming and estrogen deficiency—a critical factor in the pathogenesis of age-related OA.

The aim of this study was to evaluate the therapeutic potential of SCMs in promoting cartilage regeneration through epigenetic reprogramming in an *in vivo* model of age-related OA. Special attention was given to the structural and biochemical restoration of cartilage, as well as to the modulation of chondrocyte activity and the immune response under conditions simulating human aging and hormonal decline.

## Methods

### Laboratory animals

Experiments were performed on female white rats (*Rattus norvegicus albinus*) weighing 250–270 g. The selected animals were fertile females, classified as at least class 2 (*i.e.*, having birthed no fewer than five pups per litter),

with regular estrous cycles every 6–10 days. All animals were housed and fed under standard vivarium conditions in accordance with the recommendations of the Ethical Committee of Uzbekistan (2014) and the Ethical Guidelines for the Use of Animals in Research (2019). Ethical approval and a completed ARRIVE checklist are included in the supplementary materials.

### Study design

The experiment was conducted in two stages:

#### Stage I: Model Development

To determine the optimal inducer of knee joint OA, 34 female rats were randomly divided into four groups: three experimental groups ( $n = 8$  each) and one control group ( $n = 10$ ). Group 1 received 0.5 mL of a 10% talc suspension, Group 2 received 0.1 mL of 0.1% trypsin, and Group 3 received 0.1 mL of 1% papain. All injections were administered once intra-articularly under sterile conditions. The control group received 0.5 mL of sterile saline to account for injection-related stress.

#### Stage II: Main Experiment

Fifty-six rats were randomly allocated into six groups: Group I – Intact control ( $n = 6$ ), Group II – Intact + SCM, Group III – OA + postmenopause, Group IV – OA + postmenopause + SCM, Group V – OA + postmenopause + chondroitin sulfate, and Group VI – OA + SCM. OA was induced by intra-articular injection of trypsin. Postmenopausal state was pharmacologically modeled using clomiphene citrate (10 mg/kg/day orally, 2 courses of 5 days).

### Small chemical molecule set (SCM)

SCMs were administered intra-articularly at concentrations previously validated in *in vitro* VC6TF experiments for epigenetic reprogramming (Supplementary Table 1) [16].

### Modeling the postmenopausal state

To simulate postmenopausal conditions, clomiphene citrate—a selective estrogen receptor modulator—was used. As previously demonstrated [20], clomiphene competitively binds to estrogen receptors on chondrocytes, effectively inducing a postmenopausal-like state in experimental animals.

### Biochemical and cytokine analysis

Venous blood from the sublingual vein was collected in vacutainers with a coagulation activator (silicon dioxide), then centrifuged for 15 min at 3000 rpm. The level of cytokine expression in the serum of experimental animals was determined by the ELISA method (test systems of ZAO Vector-Best in KT-I, KT-II and KT-III). ALT and ALP on a biochemical analyzer (BioChem SA) with a built-in thermostat (High Technology, Inc). Vitamin D immunochemiluminescent assay ELISA (CTK Biotech, Inc, USA). Calcium, Phosphorus and Alkaline Phosphatase were determined by a colorimetric photometric method (Human ELISA, Germany). C-reactive protein was determined by the agglutination method (kit CRP Latex Cypress Diagnostics, Belgium)

### Histological and histochemical methods

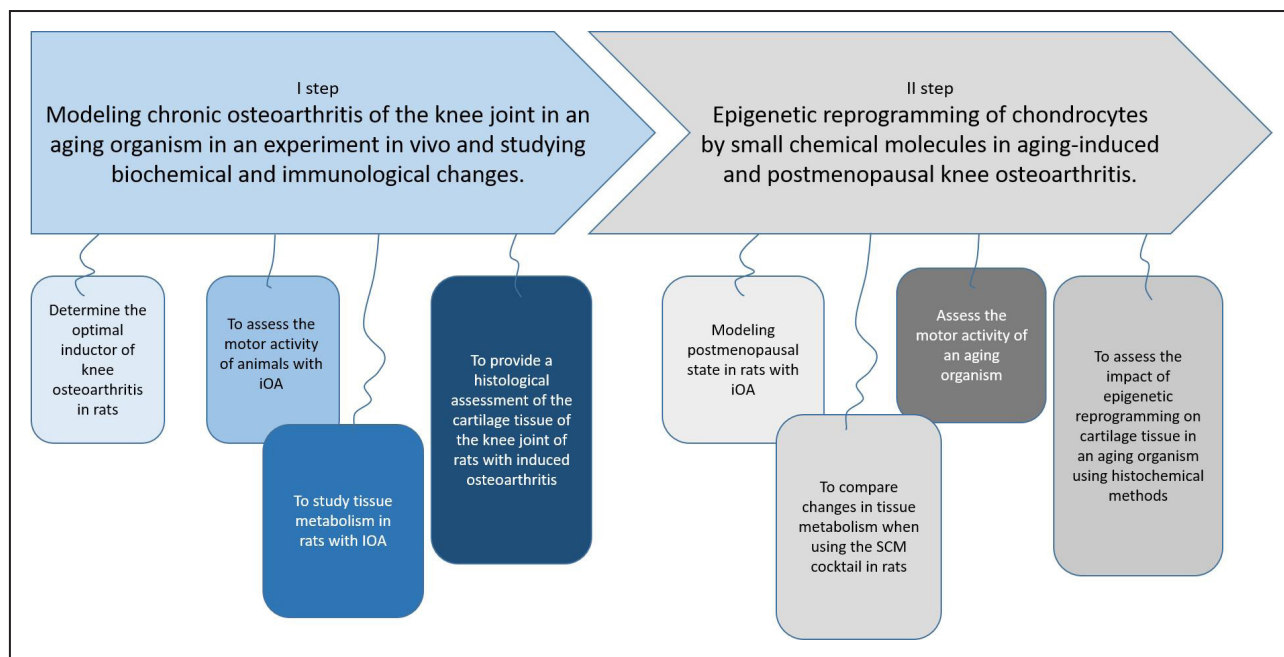


**Figure 1. General experimental design of the two-stage study.** Stage I: Optimization of the osteoarthritis (OA) model in female rats, including allocation to experimental groups, intra-articular administration of OA inducers (talc, trypsin, or papain), and subsequent clinical, biochemical, and histological assessments over a 60-day observation period. Stage II: Evaluation of small chemical molecules (SCMs) in aged rats with trypsin-induced OA, with or without estrogen receptor blockade, compared to intact controls and a chondroitin sulfate reference group. The scheme illustrates group allocation, timing of inducer and treatment administration, sampling points for biochemical and cytokine analysis, and final histological examination.

Following euthanasia, the right knee joints, including the distal femur and proximal tibia, were dissected for histomorphological analysis of cartilage and bone [24, 25]. Three staining techniques were used: hematoxylin and eosin (H&E), Van Gieson staining, and the periodic acid–Schiff (PAS) reaction. These techniques were selected to highlight structural features relevant to evaluating epigenetic reprogramming. Collected tissue samples (right lower limbs) were coded and processed group-wise. Samples were embedded in Histomix paraffin (BioVitrum, Russia), and 5–8  $\mu\text{m}$  sections were cut using a microtome. Microscopic evaluation was performed using a ZEISS Primo Star light microscope. A blinded histopathologist acquired digital microphotographs. Further image analysis was conducted using a NanoZoomer Hamamatsu system (Japan) at 50x, 100x, 200x, and 400x magnification. Digital images were captured with NanoZoomer software (REF C13140-21.S/N000198/HAMAMATSU PHOTONICS/431-3196 JAPAN). A morphometric study of tissue architecture was performed using a multiplex confocal system. The QuPath-0.5.0 software was used to generate two-dimensional images. These were analyzed along X and Y axes to calculate surface areas and lesion extent. Specific zones of articular cartilage were identified to assess the degree of tissue involvement.

#### Severity assessment: Modified Mankin scale

Cartilage degeneration was scored using the Modified Mankin scale [26], with total scores ranging from 0 (normal) to 12 (severe damage). The following parameters were assessed: surface structure (1—irregularity/erosion, 2—cracks, 3—delamination), cellularity (1—slight reduction in chondrocyte number, 2—significant reduction, 3—

complete absence), staining intensity (1—mild loss, 2—marked loss, 3—no staining), and cell proliferation (1—isogenic groups with two cells, 2—two to three cells per group, 3—proliferation foci with more than three cells per group). Nuclear–Cytoplasmic Index (N:C ratio) was measured in superficial and middle zones of the articular cartilage. For each sample, 100 chondrocytes per zone were measured using calibrated image analysis software.

#### Statistical analysis

Quantitative data were expressed as mean  $\pm$  standard deviation. Statistical analyses were performed using MS Excel 2007 and STATISTICA (Windows 10). Within-group and between-group comparisons were made using Student's t-test. For correlation analyses, Pearson's coefficient was used for normally distributed data and Spearman's rank coefficient for non-parametric data. A *P*-value of  $< 0.05$  was considered statistically significant.

## Results

To study the effect of SCM on joint tissues in OA, a series of experiments were conducted in two stages: Stage I—modeling OA in rats, and Stage II—evaluating the effect of SCMs on cartilage tissue in aged, postmenopausal rats (Figure 1).

#### Stage I: optimization of the OA model

The general scheme of the first-stage experiment is presented in [Supplementary Figure 1](#). For 60 days following the administration of OA inducers, the clinical condition of the animals was monitored, including body weight,

behavioral responses (activity, mobility, lameness, gait), functional tests (“open field” test, sprint test), and biochemical and immunological markers (calcium, phosphorus, vitamin D, alkaline phosphatase, IL-1 $\beta$ , TNF- $\alpha$ , IL-6, IL-8, and C-reactive protein).

The first clinical signs of developing gonarthrosis were observed as early as the second week, in the form of decreased activity, noticeable lameness, dragging of the right hind limb, and unsteady gait. Functional and motor activity, assessed using the “open field” and “sprint” tests, was most reduced in Group 3 (trypsin), where the lowest levels of horizontal and vertical activity, as well as movement speed, were recorded.

Among the biochemical parameters, increased serum calcium and phosphorus levels were observed in all groups with induced osteoarthritis compared to the control group. In addition, alkaline phosphatase levels were significantly elevated in the papain and trypsin groups ( $P < 0.05$ ), but not in the talc group—likely due to the presence of aluminum in talc (Supplementary Figure 2). Vitamin D concentrations remained unchanged across all groups. C-reactive protein levels significantly increased in all experimental groups ( $P < 0.05$ ), indicating an acute phase of inflammation. In this study, CRP levels rose sharply by day 30, reaching a plateau by the end of the experiment (Supplementary Figure 3).

By day 30, serum levels of IL-6 and TNF- $\alpha$  peaked in the trypsin group ( $P < 0.01$ ), reflecting an acute inflammatory response. IL-8 levels showed no significant difference in Group II (talc) compared to the control, but Groups III and IV exhibited a significant increase. A substantial elevation in IL-1 $\beta$  levels was recorded in all experimental groups (Supplementary Figure 4).

Thus, immunobiochemical analysis revealed a marked increase in proinflammatory interleukins by day 30, especially in the enzyme-induced OA groups (Groups III and IV). By day 60, however, cytokine and CRP levels stabilized, with only a slight further increase, suggesting that a stable OA phenotype had developed by day 30.

Following euthanasia, 34 rats were removed from the experiment for histomorphological examination of cartilage tissue. Histological images from the same anatomical regions in different groups were compared. Representative images are shown in Supplementary Table 2. In Group III, the medial, lateral, and central areas of the hyaline cartilage surface exhibited erosion and desquamation, along with marked chondrocyte proliferation and variable surface roughness and thickness (Supplementary Figure 5). Evidence of pannus formation was observed in the form of proliferating chondroblasts, surrounded by isogenic chondrocyte groups with uneven vacuolar degeneration. The intercellular matrix showed reduced homogeneity, with erosive-destructive changes extending to a depth of 1.025 mm. In the joint cavity, synoviocyte desquamation and accumulation of free-floating synoviocytes were observed, along with narrowing of the joint space, consistent with reactive synovitis. Dystrophic and degenerative changes were also found in the epimetaphyseal region, with resorptive cystic lesions in the metaphyseal trabeculae.

Given that spontaneous OA does not naturally develop in rats [27], it is reasonable to conclude that the observed joint damage was directly caused by OA inducer administration. Histological analysis confirmed that the most pronounced tissue alterations occurred in Groups III (trypsin) and IV (papain). These included surface erosions, fissures,

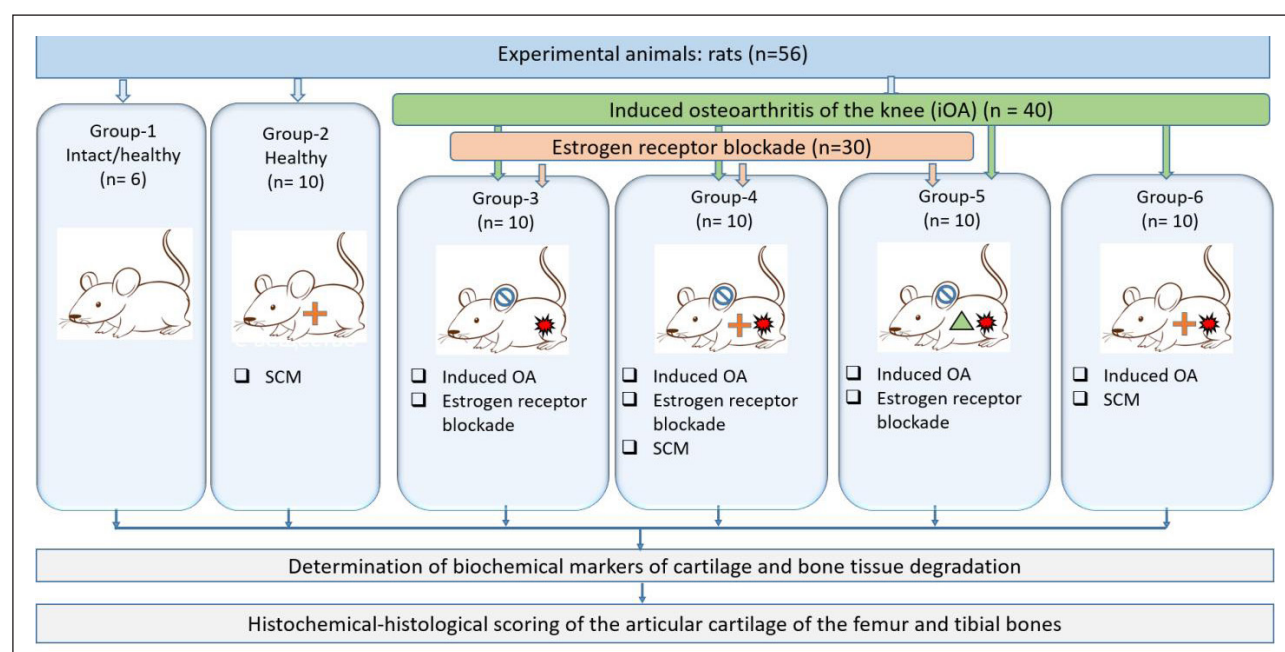


**Figure 2. Experimental design of Stage II.** Fifty-six female rats were allocated into six groups. Group I—intact control; Group II—intact + small chemical molecules (SCMs); Group III—osteoarthritis (OA) + postmenopause; Group IV—OA + postmenopause + SCMs; Group V—OA + postmenopause + chondroitin sulfate; Group VI—OA + SCMs. Treatments were administered intra-articularly following the induction of OA (trypsin) and/or estrogen receptor blockade (clomiphene citrate) where applicable. Over the 60-day observation period, clinical parameters (body weight, mobility), biochemical, cytokine profiles and histological features of the knee joint were evaluated..



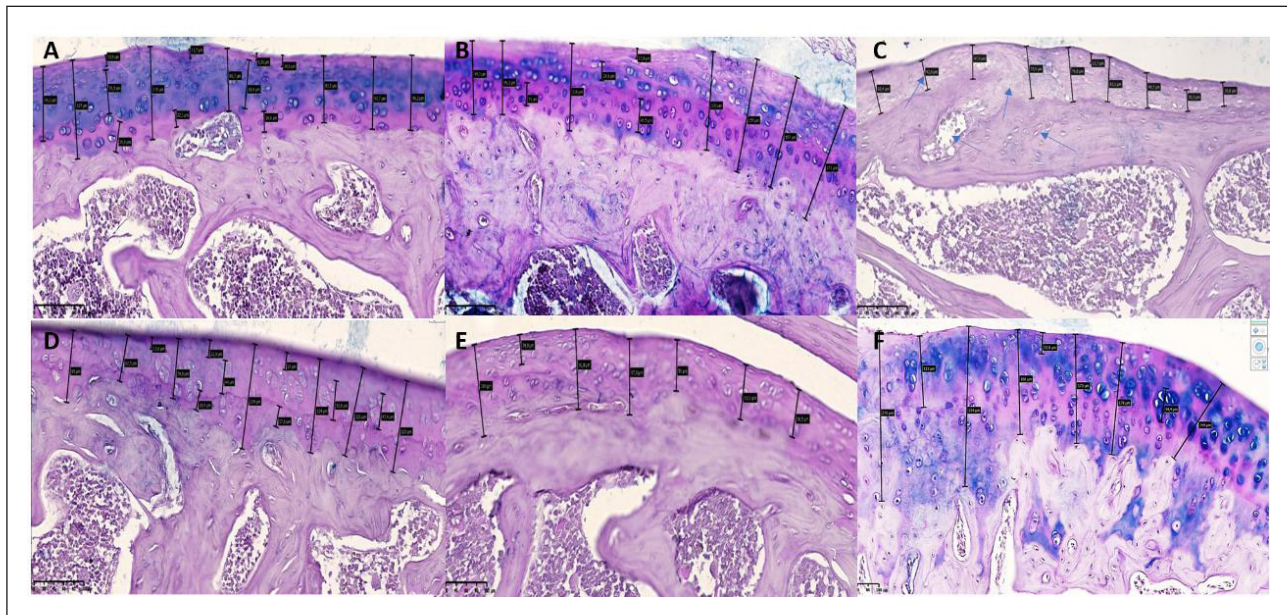


**Figure 3.** Representative histological images of articular cartilage from all experimental groups, stained with hematoxylin and eosin (H&E), periodic acid–Schiff (PAS), and Van Gieson methods. (A) Group I (Intact control) shows intact cartilage with a smooth surface and normal chondrocyte distribution. (B) Group II (Healthy + SCM) demonstrates increased mucopolysaccharide content and mild chondrocyte clustering. (C) Group III (iOA + Postmenopause) exhibits severe degeneration, deep erosions, and cystic resorption. (D) Group IV (iOA + Postmenopause + SCM) displays partial restoration of surface architecture, organized isogenic groups, and preserved extracellular matrix. (E) Group V (iOA + Postmenopause + comparison drug) shows intermediate cartilage damage with reduced PAS-positive staining. (F) Group VI (iOA + SCM) reveals uniform cartilage thickness, large isogenic chondrocyte groups, and a mucopolysaccharide-rich matrix. Arrows indicate changes in the cartilaginous tissue of the rat knee joint: uneven thickness of the surface layer; alteration in hyaline texture with disruption of the row arrangement of chondrocytes in the superficial zone; vacuolar dystrophy detected in the intermediate zone; uneven distribution of isogenic chondrocytes; presence of fibrous foci around isogenic chondrocytes; and reduced homogeneity of the interstitial substance.

ulcerations, uneven hyaline cartilage thickness, matrix vacuolization, reduced staining intensity, disrupted collagen matrix organization, and blurred zonal boundaries—findings characteristic of advanced cartilage destruction and pannus development.

Based on the extent and consistency of cartilage damage, trypsin was selected as the optimal inducer for subsequent experiments, as it most closely mimicked the chronic degenerative joint changes observed in human OA.

### Stage II: effect of SCM on aged OA model

At Stage II, 56 female rats meeting the same selection criteria as in Stage I were included in the study. All animals were divided into six groups of 10 animals each, including six intact rats (Figure 2).

Throughout the 60-day experiment, a detailed observation diary was maintained, recording the animals' body weight, motor activity, and periodic blood sampling for biochemical and immunological analyses.

### Clinical observations and weight dynamics

Body weight remained stable in Groups I and II but declined significantly in Groups III and V ( $P < 0.05$ ), correlating with behavioral signs of OA. Groups IV and VI, which received SCM, demonstrated partial preservation of body weight and motor activity (Supplementary Figure 6).

### Biochemical Parameters

ALT and AST levels were highest in Group III, reaching  $92.98 \pm 4.3$  U/L and  $366.15 \pm 18.7$  U/L, respectively. SCM treatment in Groups IV and VI significantly reduced

these enzyme levels ( $P < 0.01$ ), suggesting hepatoprotective and anti-inflammatory effects. ALP levels, which reflect bone metabolism, were significantly lower in SCM-treated groups compared to untreated OA animals ( $P < 0.05$ ).

Trypsin-induced OA significantly altered serum biochemical markers, including ALP, ALT, and AST. The elevation of these enzymes reflects activation of inflammatory pathways and a secretory phenotype in senescent cells, associated with increased cytokine and protease production.

A gradual increase in ALP was observed in the control group (Group I) over time, consistent with age-related changes. However, in SCM-treated groups (Groups II, IV, and VI), ALP levels were significantly lower ( $P < 0.05$ ), indicating a potential slowdown in both aging processes and OA progression. A similar reduction in ALP was also seen in Group III (OA + estrogen receptor blockade) (Supplementary Figure 7).

ALT and AST elevations in Group III (reaching  $92.98 \pm 4.3$  U/L and  $366.15 \pm 18.7$  U/L, respectively) were significantly reduced following SCM treatment in Groups IV and VI ( $P < 0.01$ ) (Supplementary Figures 8 & 9). A correlation was observed between ALP and ALT levels, reflecting their shared roles in bone and liver metabolism. An increase in ALT (indicating inflammation and cellular damage) was accompanied by a reduction in ALP compared to the control group, suggesting impaired bone metabolism.

Notably, the group receiving chondroitin sulfate (Group V) did not exhibit significant improvements in any of the

biochemical parameters, underscoring the need for new therapeutic strategies, particularly for postmenopausal OA.

### Cytokine profile

SCM-treated groups (Groups IV and VI) showed reduced levels of IL-1 $\beta$ , IL-6, TNF- $\alpha$ , and IL-8 compared to Group III ( $P < 0.01$ ), indicating suppression of pro-inflammatory signaling. CRP levels also declined in these groups, consistent with a reduction in systemic inflammation (Supplementary Figure 10).

### Histological assessment

Various staining methods were employed to assess cartilage integrity, including quantitative evaluation of chondrocytes and nuclear-cytoplasmic ratios. The obtained data were analyzed using the international Mankin scoring system and processed statistically. A comprehensive assessment of joint condition included key markers of chronic osteoarthritis, such as cartilage degeneration, pannus formation, joint space narrowing, synovial membrane alterations, bone tissue changes, and inflammation severity (Figure 3).

Histological analysis was conducted to evaluate the extent of cartilage degeneration and regenerative changes across all experimental groups. Group I (Intact control) displayed well-preserved cartilage with a smooth articular surface, normal zonal architecture, and evenly distributed chondro-

cytes at various stages of maturation. The cartilage matrix was dense, with no signs of erosion or pannus formation. The Mankin score was 1, indicating minimal histological alterations. Group II (Healthy + SCM) showed a slight increase in chondrocyte clustering and mucopolysaccharide content, as evidenced by intense matrix staining. Isogenic groups were aligned along a uniform trajectory within cartilage of consistent thickness. These findings suggest early anabolic activity without evident degeneration, with a Mankin score of 2. Group III (iOA + Postmenopause) exhibited the most severe histopathological changes. The cartilage surface was irregular with deep erosions and substantial chondrocyte loss. Cystic resorption cavities filled with adipose tissue were observed, and the bone trabeculae appeared thin and fragmented. Osteoclast activity was apparent, indicating advanced joint degeneration. The Mankin score was 12. Group IV (iOA + Postmenopause + SCM) demonstrated marked improvement compared to Group III. The cartilage surface was more regular, with evidence of chondrocyte proliferation and moderate vacuolar dystrophy. Isogenic clusters were organized, and the extracellular matrix was moderately preserved. The Mankin score was 4. Group V (iOA + Postmenopause + comparison drug): Showed intermediate cartilage damage. While the articular surface appeared smooth, PAS staining revealed a reduction in Schiff-positive matrix components, indicating partial degradation. Chondrocyte density was lower than in SCM-treated groups. Mankin

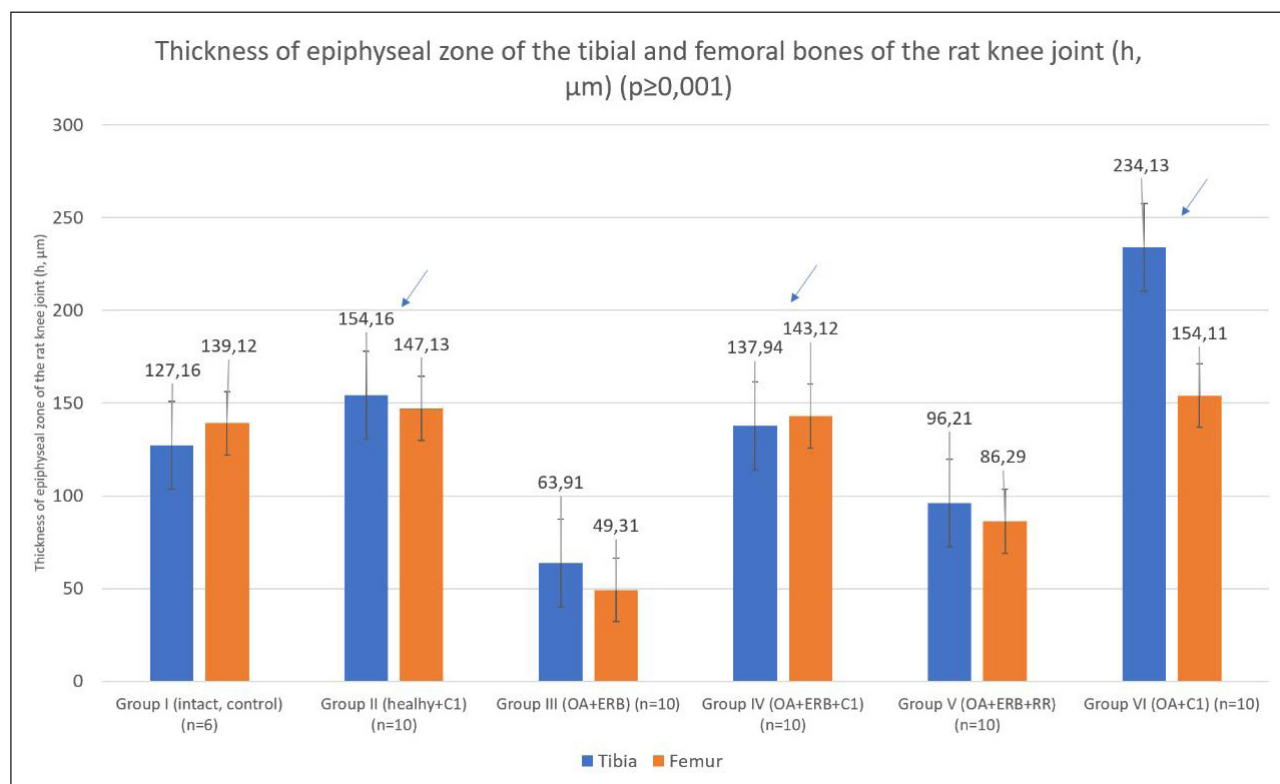


**Figure 4. Quantitative morphometric assessment of cartilage thickness and the epiphyseal zones of the tibia and femur in all experimental groups.** Measurements were performed on histological sections of the knee joint stained with hematoxylin and eosin (H&E). The analysis compared intact controls (Group I), healthy rats treated with small chemical molecules (SCMs) (Group II), and osteoarthritis (OA) models with or without postmenopausal estrogen receptor blockade and different treatments (Groups III–VI). Significant thickening of the epiphyseal cartilage was observed in SCM-treated groups (IV and VI) compared to untreated OA controls (Group III), indicating a pronounced regenerative effect of SCM administration. Data are presented as mean  $\pm$  standard deviation. Arrows indicate values significantly different from Group 3 ( $P < 0.05$ ).

score = 7. Group VI (iOA + SCM): Showed clear signs of regeneration. Cartilage layers were uniform in thickness, and large isogenic groups of chondrocytes were observed. The matrix was rich in mucopolysaccharides, suggesting enhanced biosynthetic activity. Mankin score = 6.

These histological findings confirm that SCM treatment supports chondrocyte activity and matrix repair in osteoarthritic cartilage, with particularly favorable outcomes in postmenopausal animals receiving SCM compared to untreated controls.

To enable comparative evaluation across groups, morphometric analysis and the Mankin scale were applied [26, 28]. A quantitative assessment of cartilage and epiphyseal zones in the tibia and femur was performed (Figure 4).

Notably, Group VI demonstrated significant thickening of the tibial epiphyseal zone, confirming a robust regenerative effect of SCM on OA-damaged cartilage.

To assess chondrocyte maturation, the nuclear-cytoplasmic index (NCI) was calculated in several mitotically active zones of the cartilage (Figure 5).

NCI values were significantly higher in Group I and moderately elevated in SCM-treated Groups II, IV, and VI ( $P < 0.05$  vs. Group III), indicating reactivation of chondrocyte metabolism without evidence of hyperproliferation.

Staining methods enabled the identification of cartilage damage and impaired metabolic function in OA groups, as well as restoration of metabolic activity in chondrocytes after SCM administration (Supplementary Figure 11). Group III (OA + postmenopause) showed severe cartilage degradation, including erosions, thinning, and indistinct zonal boundaries. In contrast, Groups IV and VI, which received SCM, exhibited significant histological improvement, indicating reactivation of chondrocyte metabolism.

Quantitative histological scoring ranged from 0 to 3 per parameter, with a total score from 0 (healthy tissue) to 12 (maximum cartilage damage), as summarized in Supplementary Table 3.

In our study, the lowest score (1) was observed in control Group I, while the highest (12) was recorded in untreated Group III (OA + postmenopause). Cartilage condition in Group II was slightly worse than Group I, while Group IV showed significant improvement over Group III, and Group VI demonstrated better results than Group V.

A comparative analysis across SCM-treated groups—II (Healthy + SCM), IV (OA + Postmenopause + SCM), and VI (OA + SCM)—revealed a 2:4:6 scoring pattern. This suggests a complex and possibly modulatory role of estrogen receptor blockade in postmenopausal OA (Supplementary Figure 12 and Supplementary Table 3).

Together, these findings confirm the regenerative and anti-inflammatory efficacy of SCMs in a rat model of age-related osteoarthritis.

## Discussion

We would like to emphasize that the excellent work of Yang JH *et al.* on epigenetic reprogramming using small chemical molecules (SCMs) for the rejuvenation of cell cultures inspired us to conduct this study [16]. We aimed

to obtain experimental confirmation of the effectiveness of SCMs at the organism level. Given the complexity of the cocktail's effects when administered systemically, we chose a model of joint osteoarthritis. To accurately reproduce the pathological process characteristic of age-related osteoarthritis (OA) in humans, various methods of OA modeling in animals were considered [29–31], including:

- Mechanical damage (*e.g.*, ligament rupture, meniscus removal)
- Spontaneous OA development (genetically predisposed models)
- Intra-articular administration of chemicals

A review of the literature led us to choose the intra-articular chemical induction model described in [32], as it allows us to reproduce the chronic progression of the disease, closely resembling stage III OA according to clinical classification. We used three inducers—trypsin, papain, and talc—and clinical, biochemical, and histological data confirmed that trypsin most reliably reproduces the OA phenotype. Serial measurements of biochemical and immunological parameters showed that a stable OA phenotype was established by day 30 after inducer administration. At that point, animals receiving trypsin showed significant lameness, decreased activity, and elevated levels of pro-inflammatory cytokines (IL-1 $\beta$ , IL-6, TNF- $\alpha$ ), indicating an acute inflammatory phase. CRP levels also sharply increased by day 30, plateauing thereafter. This pattern aligns with the pathogenesis of human OA, where synovial inflammation precedes cartilage degeneration and contributes to disease progression [33].

By day 60, cytokines and CRP levels did not increase exponentially but remained moderately elevated, supporting the conclusion that a stable OA phenotype had formed by day 30. Histomorphological studies revealed desquamation and erosion of hyaline cartilage in the experimental groups, with pannus formation and accumulation of freely dispersed synoviocytes. These were accompanied by joint space narrowing, indicating reactive synovitis. Since rats do not naturally develop OA [27], we attribute all observed joint changes to the chemical induction method.

At the second stage of the study, we assessed the effect of intra-articular SCMs in rats with trypsin-induced OA and estrogen deficiency. Animals receiving SCMs showed clinical improvements, including partial weight preservation and improved mobility. These improvements were accompanied by significant reductions in ALT, AST, and ALP levels, indicating decreased systemic inflammation and metabolic stress—key features of age-related OA pathophysiology [34].

SCM treatment also led to the suppression of pro-inflammatory cytokines and CRP, suggesting a decrease in senescence-associated secretory phenotype (SASP) expression [35]. This aligns with prior evidence that epigenetic modulators suppress inflammatory gene expression and restore homeostasis in senescent cells [16, 17, 36].

Histologically, SCM-treated animals exhibited smoother cartilage surfaces, restoration of isogenic chondrocyte groups, and partial matrix preservation. Epiphyseal cartilage thickness, which typically declines with age [7], was



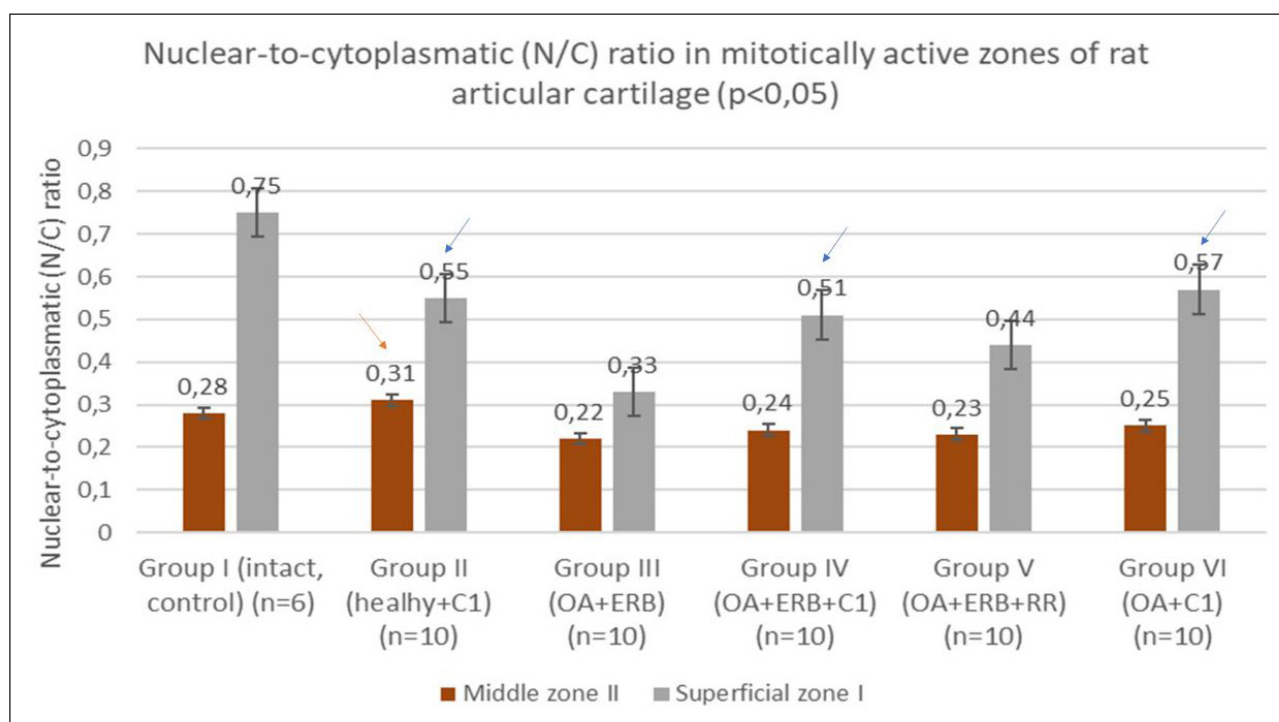


**Figure 5. Nuclear–cytoplasmic (N/C) ratio of chondrocytes in different experimental groups, calculated in mitotically active zones of the epiphyseal cartilage of the tibia and femur.** The N:C ratio was assessed on histological sections stained with hematoxylin and eosin (H&E) at  $\times 400$  magnification. Higher values indicate enhanced metabolic activation of chondrocytes. Significantly higher N:C ratios were observed in the intact control group (Group I) and in SCM-treated groups (Groups II, IV, and VI) compared to the untreated OA group (Group III), suggesting reactivation of chondrocyte metabolism without hyperproliferation. Data are presented as mean  $\pm$  standard deviation;  $P < 0.05$  versus Group III. Blue arrows indicate significant changes ( $P < 0.05$ ) in the superficial zone, and the red arrow indicates significant changes ( $P < 0.05$ ) in the median zone compared to Group III.

significantly greater in SCM-treated groups—even more than in the intact control group (Figure 4). Histochemical staining revealed intense mucopolysaccharide synthesis, indicative of heightened metabolic activity in chondrocytes. This points to epigenetic rejuvenation in vulnerable cartilage zones. Another criterion for assessing chondrocyte maturity is the nuclear-cytoplasmic index [37], which was significantly higher in SCM-treated groups compared to untreated OA groups, indicating enhanced regenerative capacity. Importantly, the NCI in SCM groups remained lower than in the control, suggesting moderate activation of mature chondrocytes without carcinogenic transformation.

According to the Mankin scale, cartilage degeneration was significantly reduced in SCM-treated groups, especially in animals with estrogen receptor blockade. Estrogen receptor- $\alpha$  (ER $\alpha$ ) not only mediates hormonal effects in cartilage but also maintains chondrocyte phenotype [38]. Blockade of ER $\alpha$  by clomiphene citrate [20] resulted in severe degeneration in untreated groups but revealed enhanced SCM efficacy in treated ones. These results indicate that estrogen receptors may play a dual role in regeneration: although their deficiency aggravates degenerative processes [39], at the same time, blockade of these receptors enhances the rejuvenating effect of SCM. This hypothesis warrants further investigation, as elucidating the mechanisms underlying the interaction between estrogens, estrogen receptors, and epigenetic reprogramming could significantly influence therapeutic strategies for treating OA in postmenopausal women.

The comparison group receiving chondroitin sulfate showed limited improvement, supporting the superiority of SCM-based epigenetic therapy over conventional symptomatic treatments.

In Groups 2, 4, and 6 (receiving SCMs), significant changes in chondrogenesis were observed. In healthy animals (Group 2), chondrocyte proliferation increased (3–5 cells per field), particularly in the upper cartilage layer. Hypercellularity of synoviocytes was also detected. Group 2 also showed decreased IL-6 and ALP levels compared to the intact Group 1, suggesting slowed aging processes. In the OA + estrogen-blockade + SCM (Group 4), cartilage destruction was less severe than in the untreated (Group 3) or chondroitin-treated (Group 5) groups. In contrast, Group 5 exhibited multifocal joint capsule destruction, erosions, and ossification—indicative of insufficient efficacy. Evidence of interstitial cartilage growth and chondrocyte mitosis in Group 4 suggests true regeneration—a rare phenomenon in aging tissues. Damage observed in these groups could be attributed to age and estrogen receptor blockade. In the untreated OA + postmenopausal group (Group 3), inflammation was highest, and histological signs of degeneration were most severe. In Group 6 (OA + SCM), regenerative changes were noted in all zones. Type I isogenic chondrocytes with large nuclei and scant cytoplasm suggested activated regenerative potential. Synoviocyte proliferation and reduced ALP levels further indicated lowered joint inflammation.

Thus, our comparative analysis of all experimental groups confirmed the high regenerative potential of SCMs *in*



*vivo.*

## Conclusions

In this study, we demonstrated that intra-articular administration of a selected set of small chemical molecules (SCMs) induces structural and metabolic restoration of cartilage tissue in a rat model of osteoarthritis (OA). By targeting epigenetic dysregulation, SCMs reduce cytokine expression, restore cartilage integrity, and improve functional outcomes. Our findings support the therapeutic potential of SCM-based epigenetic interventions for age-related OA and warrant further investigation into their clinical applications

## Declarations

**Acknowledgments:** Baratov Kuzizhon Rabbim ugli (PhD) from the Laboratory of Pharmacology and Screening of Biologically Active Substances of the Institute of Biological Chemistry of the Academy of Sciences of the Republic of Uzbekistan for assistance in working with animals; Alloberganov Dilshod Shavkatovich (PhD), Associate Professor of the Republican Center for Pathological Anatomy (Tashkent) for assistance in histological evaluation of biomaterial; Grigoryants Karina Eduardovna from the Department of Cell Therapy of the Institute of Human Immunology and Genomics (Tashkent) for assistance in photographing and videotaping experiments; Ryskulov Farukh Tursunbaevich, Department of Cell Therapy of the Institute of Human Immunology and Genomics (Tashkent) for assistance in conducting laboratory work.

**Authors contribution:** Saodat Muratkhodjaeva performed all experimental work, mathematical data processing and graphs, and made significant contributions to the writing of the manuscript. Tamara Aripova was responsible for the overall supervision of the experiments and writing the manuscript. Javdat Muratkhodjaev was responsible for the overall idea and writing of this manuscript. All authors read and approved the final version of the manuscript and take accountability for all aspects of the work, ensuring that questions related to the accuracy or integrity of any part of the work are appropriately investigated and resolved.

**Financial support and sponsorship:** None.

**Conflicts of interest:** All authors declared that there are no conflicts of interest.

**Ethical approval and consent to participate:** All animal studies were conducted in accordance with the recommendations of the Ethics Committee of Uzbekistan (2014) and the Ethical Guidelines for the Use of Animals in Scientific Research (2019). The Ethics Committee's permission to work with laboratory animals and the completed ARRIVE checklist are attached.

## References

1. Yang J, Hayano M, Griffin P, Amorim J, Bonkowski M, Apostolides J, *et al.* Loss of epigenetic information as a cause of mammalian aging. *Cell*, 2023, 186(2): 305-326. e327. [\[Crossref\]](#)
2. López-Otín C, Blasco M, Partridge L, Serrano M, & Kroemer G. The hallmarks of aging. *Cell*, 2013, 153(6): 1194-1217. [\[Crossref\]](#)
3. Pal S, & Tyler J. Epigenetics and aging. *Sci Adv*, 2016, 2(7): e1600584. [\[Crossref\]](#)
4. Lu Y, Tian X, & Sinclair D. The information theory of aging. *Nature Aging*, 2023, 3(12): 1486-1499. [\[Crossref\]](#)
5. Guo J, Huang X, Dou L, Yan M, Shen T, Tang W, *et al.* Aging and aging-related diseases: from molecular mechanisms to interventions and treatments. *Signal Transduct Target Ther*, 2022, 7(1): 391-405. [\[Crossref\]](#)
6. Diekmann B, & Loeser R. Aging and the emerging role of cellular senescence in osteoarthritis. *Osteoarthritis Cartilage*, 2024, 32(4): 365-371. [\[Crossref\]](#)
7. Loeser R. Aging and osteoarthritis: the role of chondrocyte senescence and aging changes in the cartilage matrix. *Osteoarthritis Cartilage*, 2009, 17(8): 971-979. [\[Crossref\]](#)
8. Croft A, Campos J, Jansen K, Turner J, Marshall J, Attar M, *et al.* Distinct fibroblast subsets drive inflammation and damage in arthritis. *Nature*, 2019, 570(7760): 246-251. [\[Crossref\]](#)
9. Long H, Liu Q, Yin H, Wang K, Diao N, Zhang Y, *et al.* Prevalence trends of site-specific osteoarthritis from 1990 to 2019: findings from the global burden of disease study 2019. *Arthritis Rheumatol*, 2022, 74(7): 1172-1183. [\[Crossref\]](#)
10. Global, regional, and national burden of osteoarthritis, 1990-2020 and projections to 2050: a systematic analysis for the global burden of disease study 2021. *Lancet Rheumatol*, 2023, 5(9): e508-e522. [\[Crossref\]](#)
11. Ushiyama T, Ueyama H, Inoue K, Ohkubo I, & Hukuda S. Expression of genes for estrogen receptors alpha and beta in human articular chondrocytes. *Osteoarthritis Cartilage*, 1999, 7(6): 560-566. [\[Crossref\]](#)
12. Nüesch E, Dieppe P, Reichenbach S, Williams S, Iff S, & Jüni P. All cause and disease specific mortality in patients with knee or hip osteoarthritis: population based cohort study. *Bmj*, 2011, 342: d1165. [\[Crossref\]](#)
13. Wehling P, Evans C, Wehling J, & Maixner W. Effectiveness of intra-articular therapies in osteoarthritis: a literature review. *Ther Adv Musculoskelet Dis*, 2017, 9(8): 183-196. [\[Crossref\]](#)
14. Berenbaum F. Annals of the Rheumatic Diseases collection on osteoarthritis (2018-2023): hopes and disappointments. *Ann Rheum Dis*, 2024, 83(2): 133-135. [\[Crossref\]](#)
15. Ball H, Alejo A, Kronk T, Alejo A, & Safadi F. Epigenetic regulation of chondrocytes and subchondral bone in osteoarthritis. *Life (Basel)*, 2022, 12(4): 582-593. [\[Crossref\]](#)
16. Yang J, Petty C, Dixon-McDougall T, Lopez M, Tyshkovskiy A, Maybury-Lewis S, *et al.* Chemically induced repro-

- gramming to reverse cellular aging. *Aging (Albany NY)*, 2023, 15(13): 5966-5989. [[Crossref](#)]
17. Pereira B, Correia F, Alves I, Costa M, Gameiro M, Martins A, *et al.* Epigenetic reprogramming as a key to reverse ageing and increase longevity. *Ageing research reviews*, 2024, 95: 102204. [[Crossref](#)]
  18. Knyazer A, Bunu G, Toren D, Mracica T, Segev Y, Wolfson M, *et al.* Small molecules for cell reprogramming: a systems biology analysis. *Aging*, 2021, 13(24): 25739-25762. [[Crossref](#)]
  19. Nie B, Nie T, Hui X, Gu P, Mao L, Li K, *et al.* Brown adipogenic reprogramming induced by a small molecule. *Cell Rep*, 2017, 18(3): 624-635. [[Crossref](#)]
  20. Kalashnikova S, & V.V N. Estrogens and modulation of the hypothalamic-pituitary-thyroid axis during chronic endogenous intoxication in rats. *Bulletin of the Volgograd Scientific Center of the Russian Academy of Medical Sciences*, 2009, 1(21): 49-53.
  21. Corciulo C, Scheffler J, Gustafsson K, Drevinge C, Humeniuk P, Del Carpio Pons A, *et al.* Pulsed administration for physiological estrogen replacement in mice. *F1000Res*, 2021, 10: 809-812. [[Crossref](#)]
  22. Ge Y, Zhou S, Li Y, Wang Z, Chen S, Xia T, *et al.* Estrogen prevents articular cartilage destruction in a mouse model of AMPK deficiency via ERK-mTOR pathway. *Ann Transl Med*, 2019, 7(14): 336-345. [[Crossref](#)]
  23. Horkeby K, Farman H, Movérare-Skrtic S, Lionikaite V, Wu J, Henning P, *et al.* Phosphorylation of S122 in ER $\alpha$  is important for the skeletal response to estrogen treatment in male mice. *Sci Rep*, 2022, 12(1): 22449. [[Crossref](#)]
  24. Gyarmati J, Földes I, Kern M, & Kiss I. Morphological studies on the articular cartilage of old rats. *Acta Morphol Hung*, 1987, 35(3-4): 111-124.
  25. Mankin H, Dorfman H, Lippiello L, & Zarins A. Biochemical and metabolic abnormalities in articular cartilage from osteoarthritic human hips. II. Correlation of morphology with biochemical and metabolic data. *J Bone Joint Surg Am*, 1971, 53(3): 523-537.
  26. Moody H, Heard B, Frank C, Shrive N, & Oloyede A. Investigating the potential value of individual parameters of histological grading systems in a sheep model of cartilage damage: the Modified Mankin method. *J Anat*, 2012, 221(1): 47-54. [[Crossref](#)]
  27. Kalbhen D. Chemical model of osteoarthritis--a pharmacological evaluation. *J Rheumatol*, 1987, 14 Spec No: 130-131.
  28. Yeh T, Wen Z, Lee H, Lee C, Yang Z, Jean Y, *et al.* Intra-articular injection of collagenase induced experimental osteoarthritis of the lumbar facet joint in rats. *Eur Spine J*, 2008, 17(5): 734-742. [[Crossref](#)]
  29. Salo P, Hogervorst T, Seerattan R, Rucker D, & Bray R. Selective joint denervation promotes knee osteoarthritis in the aging rat. *J Orthop Res*, 2002, 20(6): 1256-1264. [[Crossref](#)]
  30. Muzhikyan A, Shekunova E, Kashkin V, Makarova M, & Makarov V. Histological evaluation of joint pathology in various models of chronic arthritis in rats. *Laboratornye Zhivotnye dlya nauchnykh issledovaniy (Laboratory Animals for Science)*, 2018, 1: 04. [[Crossref](#)]
  31. Korochina K, Chernysheva T, Polyakova VS, & Korochina I. Features of morphology of articular cartilage in patients with different phenotypes of knee osteoarthritis. *Arkhiv patologii*, 2020, 82: 13-25. [[Crossref](#)]
  32. Perepelkina D, Nasibova S, Bakhtin V, & N.V I (2019). Histological technique for preparing articular cartilage preparations from laboratory animals. Proceedings of V International (75<sup>th</sup> All-Russian) Scientific and Practical Conference "Topical Issues of Modern Medical Science and Healthcare.
  33. Sanchez-Lopez E, Coras R, Torres A, Lane N, & Guma M. Synovial inflammation in osteoarthritis progression. *Nat Rev Rheumatol*, 2022, 18(5): 258-275. [[Crossref](#)]
  34. Loeser R, Collins J, & Diekman B. Ageing and the pathogenesis of osteoarthritis. *Nat Rev Rheumatol*, 2016, 12(7): 412-420. [[Crossref](#)]
  35. Cuollo L, Antonangeli F, Santoni A, & Soriani A. The senescence-associated secretory phenotype (SASP) in the challenging future of cancer therapy and age-related diseases. *Biology*, 2020, 9(12): 485-496. [[Crossref](#)]
  36. Zhu X, Chen Z, Shen W, Huang G, Sedivy J, Wang H, *et al.* Inflammation, epigenetics, and metabolism converge to cell senescence and ageing: the regulation and intervention. *Signal Transduct Target Ther*, 2021, 6(1): 245-255. [[Crossref](#)]
  37. Pritzker K, Gay S, Jimenez S, Ostergaard K, Pelletier J, Revell P, *et al.* Osteoarthritis cartilage histopathology: grading and staging. *Osteoarthritis Cartilage*, 2006, 14(1): 13-29. [[Crossref](#)]
  38. Zhang X, Xiang S, Zhang Y, Liu S, Lei G, Hines S, *et al.* In vitro study to identify ligand-independent function of estrogen receptor- $\alpha$  in suppressing DNA damage-induced chondrocyte senescence. *Faseb j*, 2023, 37(2): e22746. [[Crossref](#)]
  39. Wang N, Zhang X, Rothrauff B, Fritch M, Chang A, He Y, *et al.* Novel role of estrogen receptor- $\alpha$  on regulating chondrocyte phenotype and response to mechanical loading. *Osteoarthritis Cartilage*, 2022, 30(2): 302-314. [[Crossref](#)]

**Cite this article as:** Muratkhodjaeva SA, Muratkhodjaev JN, & Aripova TU. Experimental confirmation of osteoarthritis repair *in vivo* using epigenetic reprogramming with small molecules. *Aging Pathobiol Ther*, 2025, 7(3): xx-xx. doi:10.31491/APT.2025.09.xxx

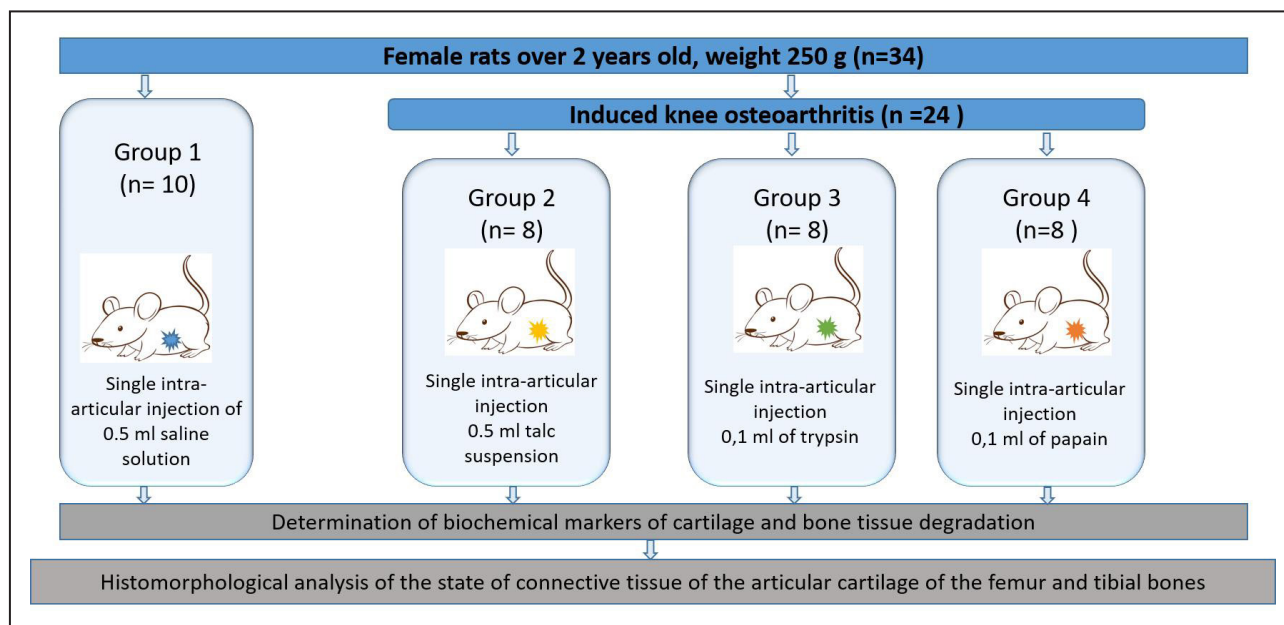


**Figure S1.** Design of experiments to verify the model of induced osteoarthritis in rats.

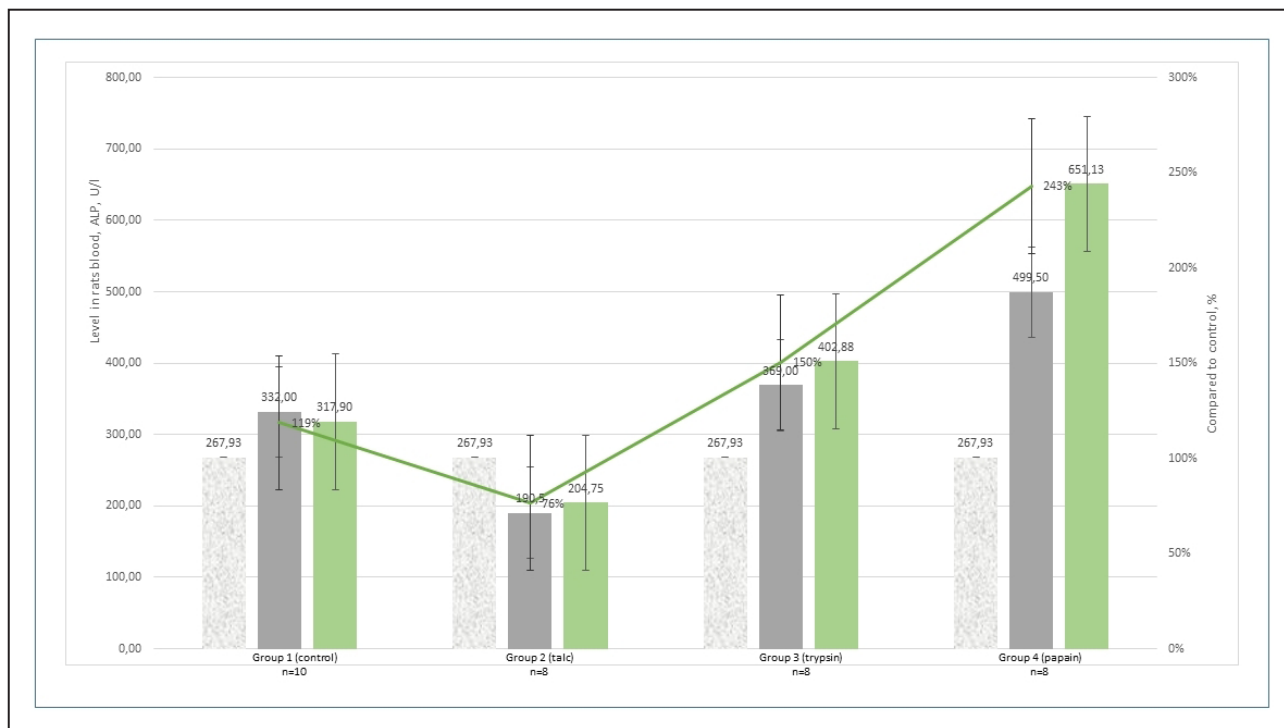


**Figure S2.** Blood alkaline phosphatase levels in rats with induced osteoarthritis on day 60 of the experiment.



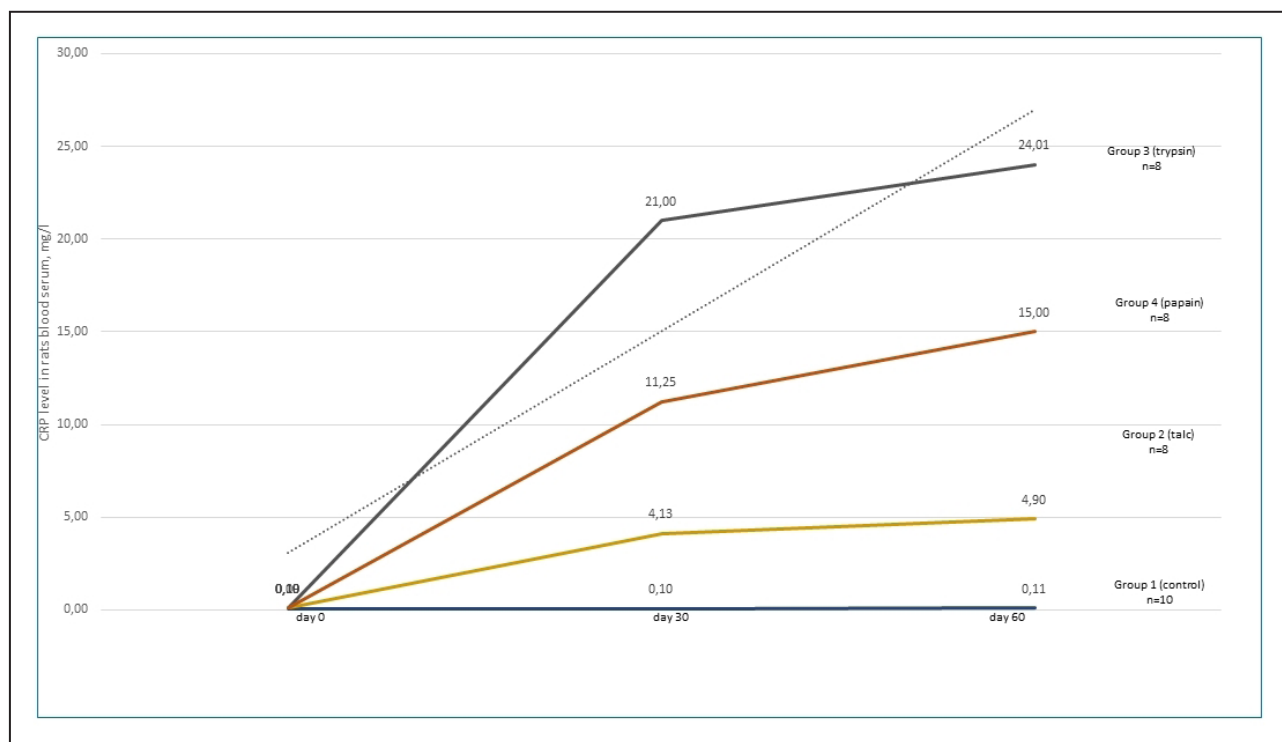


Figure S3. Dynamics of changes in the level of C-reactive protein in rats blood serum.

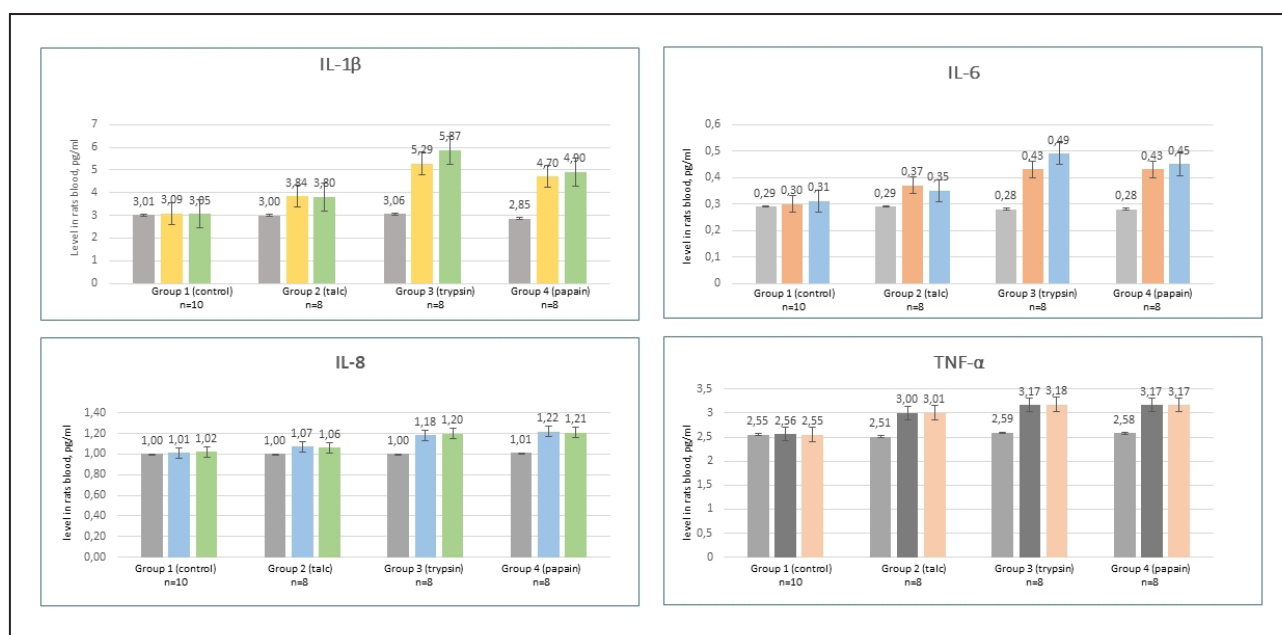
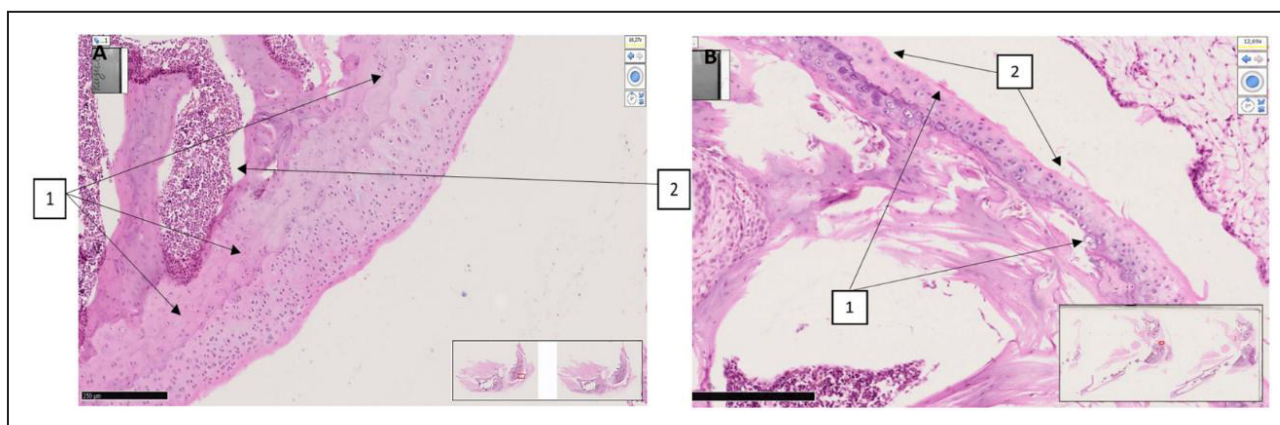
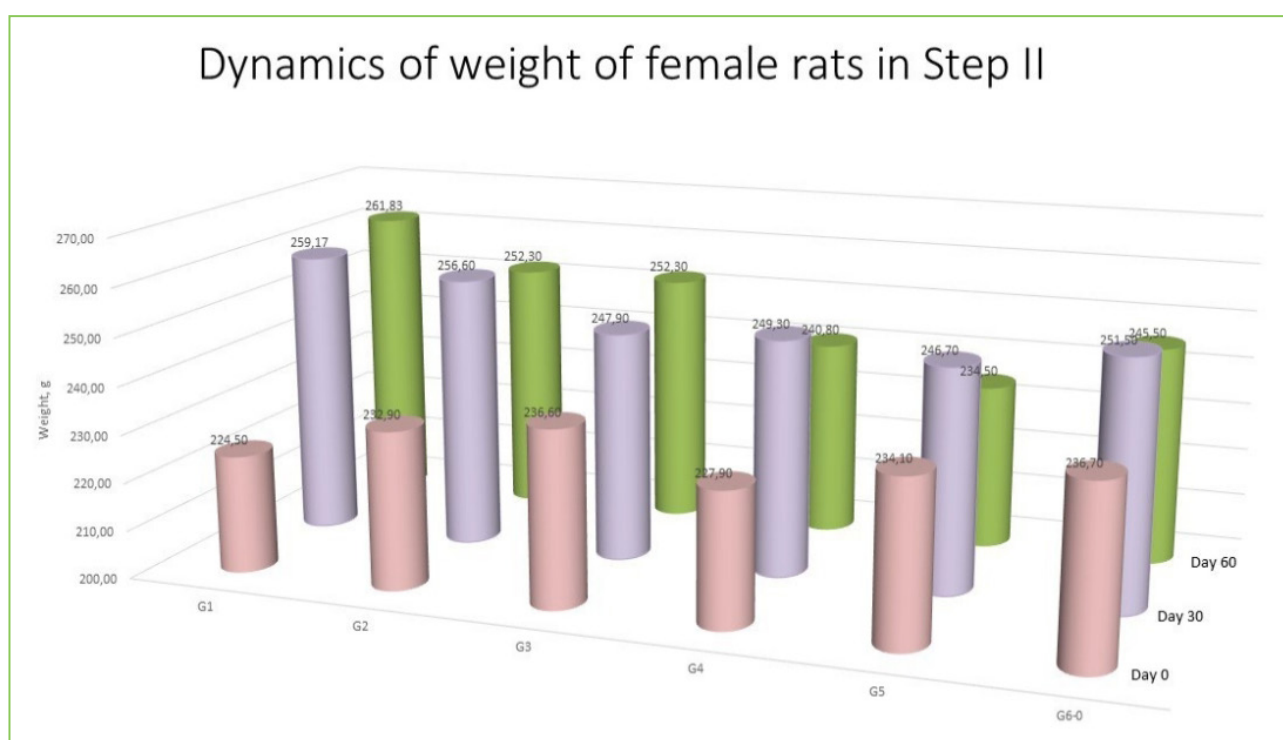


Figure S4. Cytokine profile indicators in rats blood serum.



**Figure S5. Characteristic histomorphological sections of the rat knee joint.** (A) Knee joint of rat (first group with red mark). On the medial-lateral surface of the epiphyseal surface of the femur, the surface of the hyaline cartilage is somewhat uneven, the thickness of the hyaline plate is greater than usual, in the thickness of the plate near the basal layer, unevenly wavy myxomatous foci are revealed. (1). Red bone marrow is found in the metaphyseal region (2). H&E stain. Magnifications 10x10. (B) Knee joint of a rat (inducer trypsin). Sharp destructive and disregenerative changes are revealed on the lateral and medial-lateral surface of the hyaline surface of the knee joint (1), erosive-desquamative foci are revealed on the surface of the hyaline coating (2). H&E stain. Magnifications 10x10. The morphofunctional state of the knee joints of rats in the group with trypsin-induced osteoarthritis was determined at a level of 12 points on the Mankin scale. There are destructive and dysregenerative changes, damage to the components of the hyaline cartilage. As a result of microscopic examinations, symptoms of reactive synovitis and reactive arthritis were determined. This indicator indicates that the level of traumatism is very high, and the model used in the experimental conditions is recognized as highly effective in terms of alternative impact in this group.



**Figure S6.** Weight of rats during experiments.

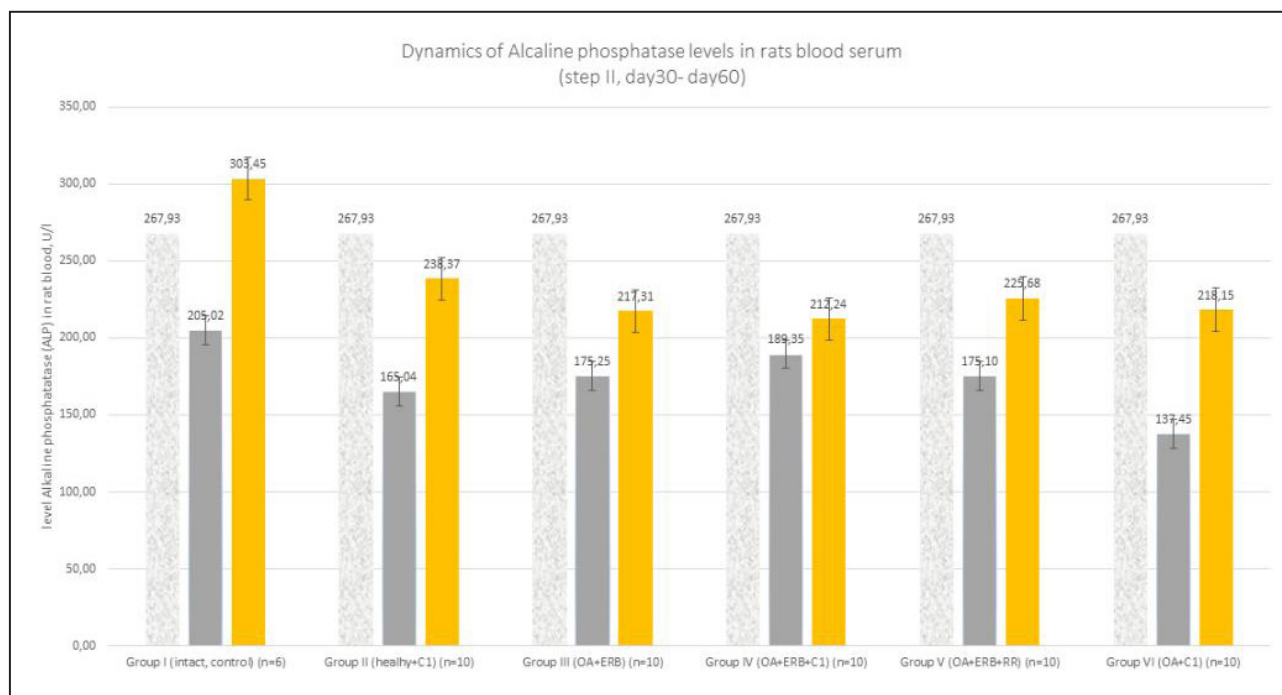


Figure S7. Dynamics of alkaline phosphatase levels in rats blood serum.

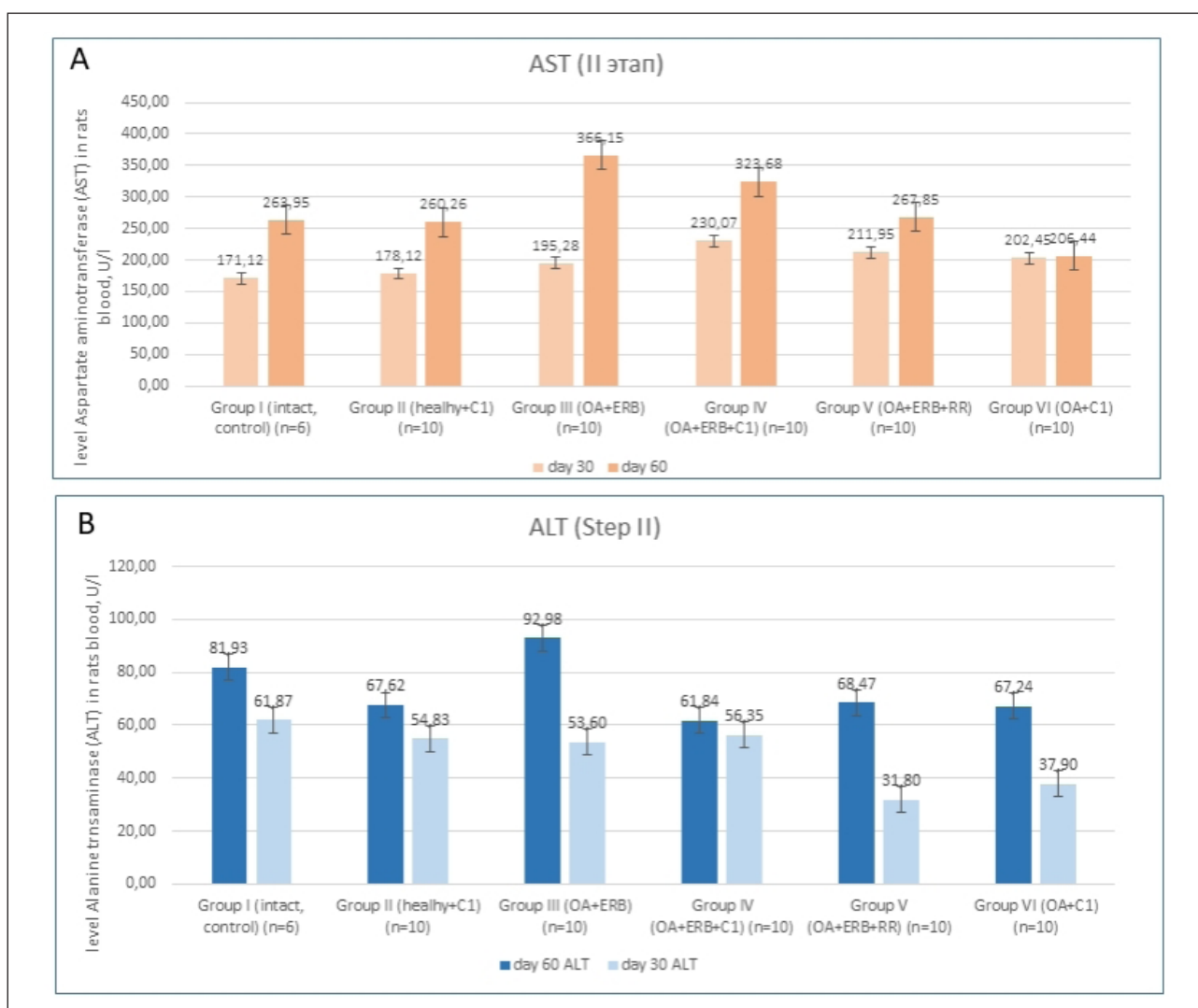


Figure S8. Dynamics of changes in enzymes in rats blood serum. (A) AST level. (B) ALT level.



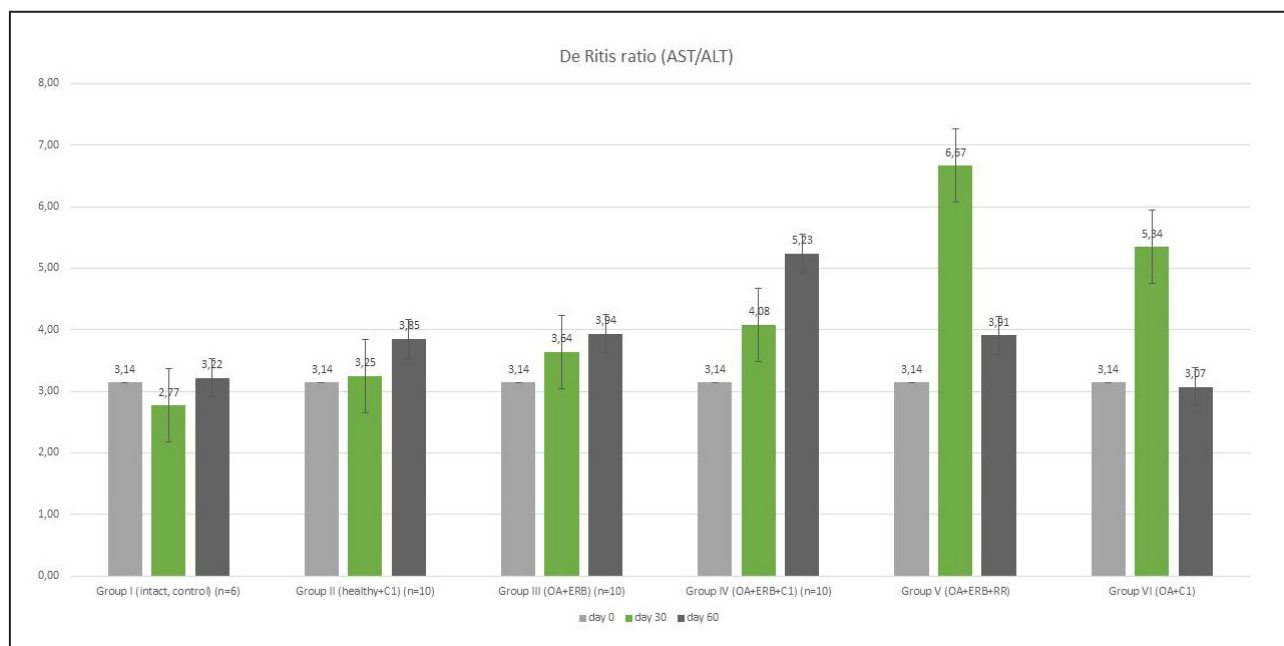


Figure S9. Ratio of AST and ALT levels.

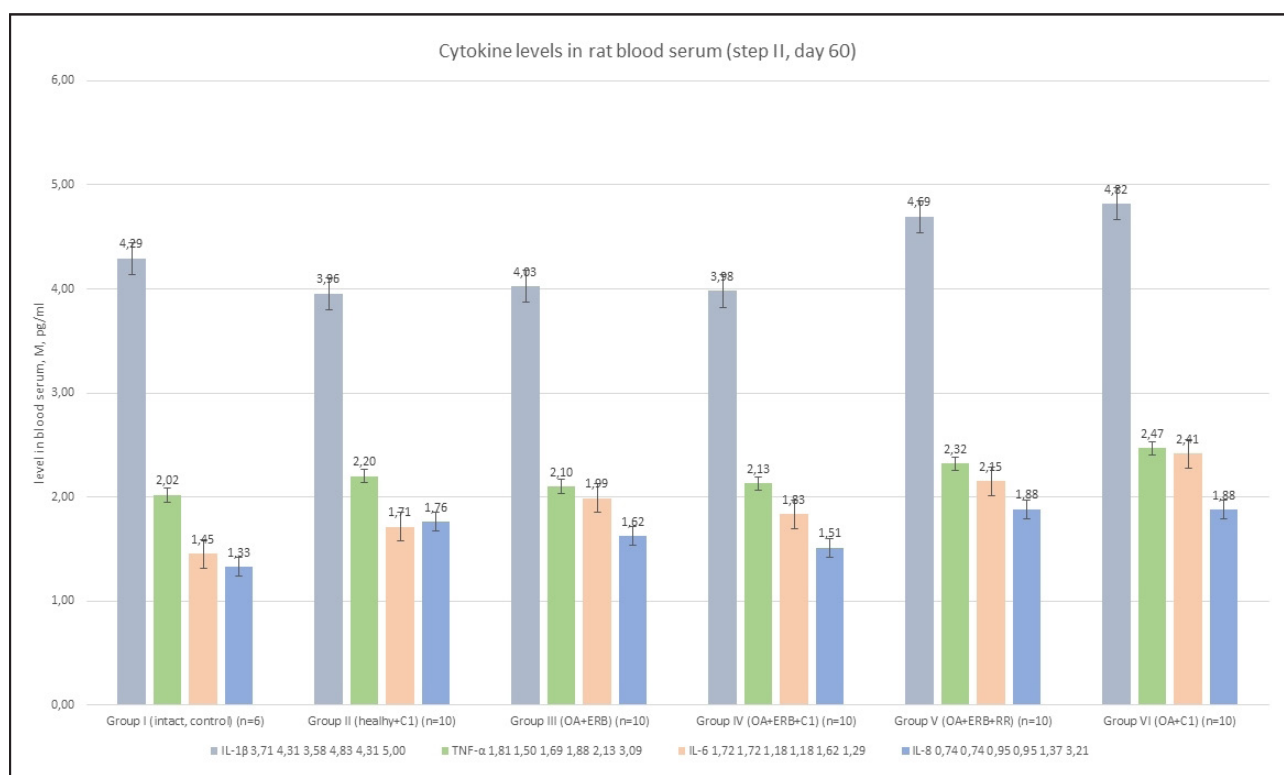
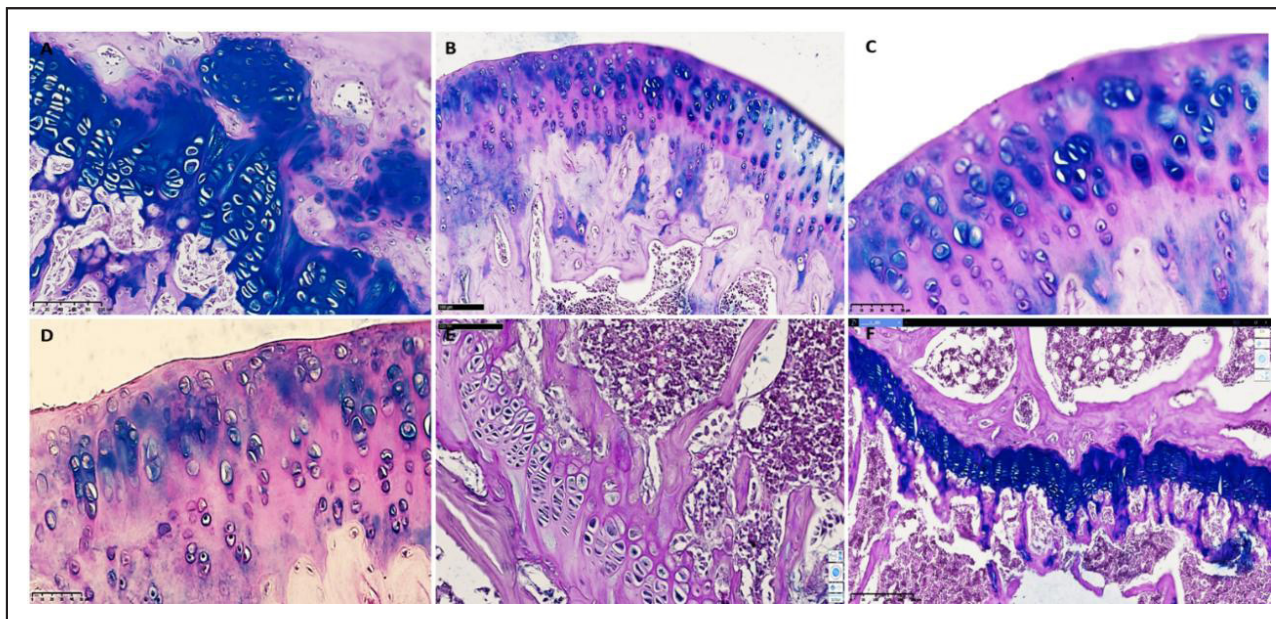
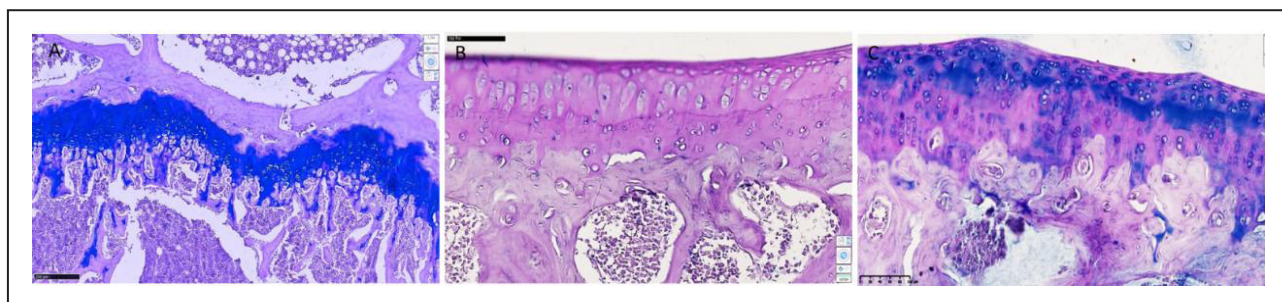


Figure S10. Cytokine levels in rats blood serum.



**Figure S11. Comparison of the rat groups with knee induced osteoarthritis and estrogen receptor blockade.** (A) Group III (iOA + estrogen receptor blockade). of rats: epimetaphyseal region of the knee joint. It was found that the border of isogenic chondrocytes is shifted to the metaphyseal region, and the epimetaphyseal zone is invaginated to the subepiphyseal branch. SCHIFF-positive dark blue structures are found around chondrocytes with vacuolar dystrophy and signs of necrobiosis. Magn. 20x10. Dystrophic and disreenerative, destructive changes are revealed in bone beams. The number of osteoblasts is small, osteoclasts are increased, this process means the expansion of bone pores and the formation of resorptive cysts of enlarged foci. Cystically expanded resorption spaces indicate the development of osteoporosis processes. In the area of the joint pockets, highly developed interstitial formations with a small number of interstitial macrophages are found. (B) Group IV (iOA + estrogen receptor blockade + SCM). The surface of the knee joint of rats of the 4th group. The surface of the joint is relatively smooth, in all rows of the hyaline cartilage cover chondrocytes in a state of proliferation and hypertrophy are found, and also, in focus were chondrocytes with vacuolar dystrophy. Isogenic chondrocytes are grouped and located relatively orderly. H&E stain. Magnifications 20x10. Isogenic chondrocytes are arranged in an orderly manner, their number is 9-12 in a 200x field of view. Foci of acute proliferation of chondroblasts are revealed, cells of the isogenic group of chondrocytes have focal vacuolar dystrophy, the extracellular matrix is homogenized, the cell nuclei are stained with a basophilic dye, have a relatively uniform appearance, which indicates restored metabolic processes. (C) Group V (iOA + estrogen receptor blockade + comparison drug). The surface of the knee joint of rats of the 5th group. The surface of the joint is relatively uneven, proliferation and hypercellular appearance are observed, multifocal vacuolar dystrophy of all rows of chondrocytes in the hyaline cartilage cover. Isogenic chondrocytes are grouped and located relatively unevenly. H&E stain Magnifications 20x10. In this group, changes were observed due to multifocal destruction of the components of the joint capsule, accumulation of pyramidal lacunae of chondrocytes of different sizes around collagen fibers. On the surface of the joints, foci of erosion measuring 0.24-0.36 mm, foci of ossification in the epimetaphyseal layer of hyaline cartilage and uneven texture of the basement membrane were noted. (D) Group III (iOA + estrogen receptor blockade). Surface of the rat knee joint. The joint surface is uneven, chondrocytes in all rows are of different sizes, with signs of vacuolar dystrophy. Isogenic chondrocytes are unevenly distributed. H&E stain Magnifications 40x10. There are foci of reparative regeneration of chondrocytes at different stages, in other areas thickenings and uneven surfaces are formed. There is very little extracellular matrix around isogenic chondrocytes, instead of it fibrous foci of coarse collagen fibers are determined. Focuses of reparative regeneration of chondrocytes at different stages are observed, in other areas thickenings and uneven surfaces are formed. In the deep layer of radial arrangement of chondrocytes, they have a hypertrophied appearance, semi-oval shape, oblong in places, are located in a disorderly manner, 3-9 groups are visible. Chondrocyte groups are subject to uneven vacuolar degeneration, the homogeneity of the interstitial substance is relatively reduced, the basophilic coloration of the cells is different, which indicates a metabolic disorder. Around chondrocytes in the state of necrobiosis and necrosis, proliferation of fibroblasts and an increase in coarse collagen fibers are observed. (E) Group IV (iOA + estrogen receptor blockade + SCM). Rat knee joint. Epimetaphyseal region has thinned flat textured appearance, isogenic chondrocytes of the same size in the area of transition to bone trabeculae, same appearance, bone trabeculae are thickened. H&E stain. Magnifications 4x10. No changes in the structure of the ligaments and tendons of the joint muscles were detected. In the epimetaphyseal zone, the isogenic chondrocytes are of the same size, the ossification boundary and the trajectory of the metaphyseal zone have the same arcuate shape, no sharp thickened zones are determined. In the epimetaphyseal and metaphyseal regions, the bone beams are of the same thickness, osteoblasts are clearly defined, their number is increased by 1.25 times, the bone beams are uniformly thickened compared to the norm, the proliferative activity of osteoblasts is increased. (F) Group V (iOA + estrogen receptor blockade + comparison drug). Epimetaphyseal branch of the knee joint of rats of the 5th group. The border of isogenic chondrocytes varies from the metaphyseal branch to the superficial layer of the bone, multifocal vacuolar dystrophy and necrobiosis in isogenic chondrocytes are revealed around them. SCHIFF-positive method. Magnifications 20x10. The structure of isogenic chondrocytes in the upper and middle sections of the hyaline layer is changed, the lacunae have a pyramidal appearance, the cells have multifocal hydropic dystrophy, and pericellular edema is detected around them. The adoption of a rounded shape by chondrocytes in this area is explained by the fact that the apoptosis process is intensified. According to histochemical tests, it was established that Schiff-positive structures are reduced, metabolism is enhanced, and the number of intermediate products is sharply reduced.



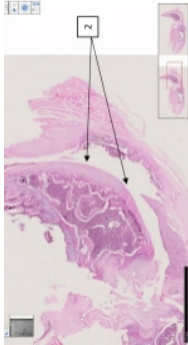
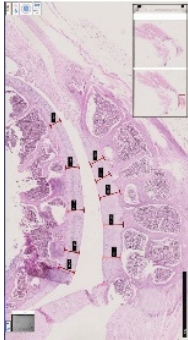
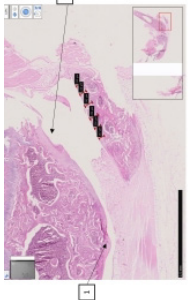
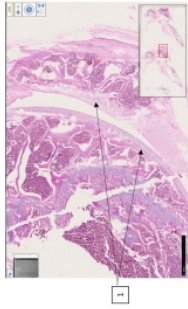
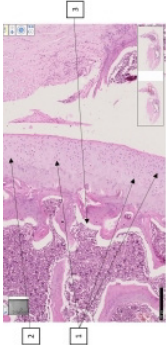
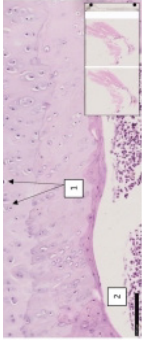
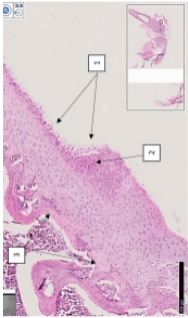
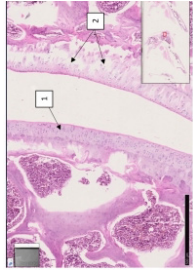
**Figure S12. Comparison of groups of rats treated with SCM.** (A) Group II (healthy animals and SCM). Isogenic chondrocytes on the articular surface and epimetaphyseal plate form SCHIFF-positive structures of uniform appearance. Schiff-positive structures are found in small quantities in the meniscus and patella. The bone beams in the metaphyseal zone have the same thickness, osteoblasts have a normal appearance, the sizes of the cavities of the spongy substance have the same width. No significant changes were found in other components of the knee joint. (B) Group IV (trypsin induced knee OA with Estrogen receptor blockade and SCM). Necrobiosis and necrotic chondrocytes are detected in small quantities only. Fibroblast proliferation and synthesis of coarse fibrous collagen are detected only in the subchondral and epimetaphyseal branches. Along the perimeter of the joint, in the pockets of the inner surface of the capsule, disorganization and destructive changes are not detected. On the inner surface of the synovial membrane of the joint, focal hyperplasia of synoviocytes and an increase in regeneration indicators are determined. The joint space is normal in appearance, not damaged, the menisci have the same homogeneous consistency, pathological changes in the structures of hyaline and collagen fibers are not detected. (C) Group VI (trypsin induced knee OA and SCM). PAS-stained micrographs show focal accumulations of acid mucopolysaccharides, predominantly around the perimeter of chondrocytes and fibroblasts, with pale blue PAS-positive structures. Acid mucopolysaccharides are produced by hyaline chondrocytes and fibroblasts and occur in various forms. The proliferative changes of varying degrees were observed in chondrocytes, as well as the formation of foci of osteofibrosis and calcification instead of foci of osteonecrosis and osteoporosis.

**Table S1.** Composition and concentrations of small chemical molecule (SCM) cocktail.

	Name	Final concentration (μM)	Solvent	Source& catalog No
1	Valproic acid (VPA)	250	water	Sigma-Aldrich P4543-25G
2	CHIR99021	10	DMSO	Sigma-Aldrich SML1046-5MG
3	E-616452 (Repsox)	10	DMSO	Sigma-Aldrich R0158-5MG
4	Tranylcypromine	5	water	Merck 616431-500MG
5	Forskolin (FSK)	50	DMSO	Sigma-Aldrich F6886-10MG



Table S2. Comparative histological representation of knee joint tissues in rats with chemically induced osteoarthritis

Knee joint area	Group I (n = 10)	Group II (n = 8)	Group III (n = 7)	Group IV (n = 8)
Synovial cleft and surface of the knee joint of the femur. Staining H-E.				
Lateral and medial-lateral surface of the femur. H.-E. Magnifications 10x10				

**Table S3.** The severity of cartilage degeneration in different groups according to the modified Mankin scale with a range of scores from 0 (normal) to 3 (severe degeneration).

Modified Mankin scale							
No.	Histological parameter	Group I	Group II	Group III	Group IV	Group V	Group VI
1	Surface structure (1 point – unevenness, erosion; 2 points – cracks; 3 points – delamination)	0	0	3	1	2	2
2	Cellular composition (1 point - slight decrease in the number of chondrocytes; 2 points - significant decrease in the number of chondrocytes; 3 points - no cells)	0	0	3	1	1	1
3	Staining (1 point - slight decrease in staining; 2 points - significant decrease in staining; 3 points - no staining)	0	0	3	0	1	0
4	Cell proliferation (1 point - isogenic groups of chondrocytes with 2 cells per group; 2 points - isogenic groups with 2-3 cells per group; 3 points - foci of proliferation (more than 3 cells per group).	1	2	3	2	3	3
Total		1	2	12	4	7	6